

Unconventional level attraction in cavity axion polariton of antiferromagnetic topological insulator

Yang Xiao^{1,*}, Huaiqiang Wang^{2,3,*}, Dinghui Wang², Ruifeng Lu⁴, Xiaohong

Yan⁵, Hong Guo⁶, C. -M. Hu⁷, Ke Xia⁸, Haijun Zhang^{2,3,†} and Dingyu Xing^{2,3}

¹College of Science, Nanjing University of Aeronautics and Astronautics, Nanjing 210016, China

²National Laboratory of Solid State Microstructures and Physics School, Nanjing University, Nanjing 210093, China

³Collaborative Innovation Center of Advanced Microstructures, Nanjing University, Nanjing 210093, China

⁴Department of Applied Physics, Nanjing University of Science and Technology, Nanjing 210094, China

⁵School of Material Science and Engineering, Jiangsu University, Zhenjiang, 212013, China

⁶Department of Physics, McGill University, Montreal, Quebec H3A 2T8, Canada

⁷Department of Physics and Astronomy, University of Manitoba, Winnipeg R3T 2N2, Canada and

⁸Beijing Computational Science Research Center, Beijing 100193, China*

Strong coupling between cavity photons and various excitations in condensed matters boosts the field of light-matter interaction and generates several exciting sub-fields, such as cavity optomechanics and cavity magnon polariton. Axion quasiparticles, emerging in topological insulators, were predicted to strongly couple with the light and generate the so-called axion polariton. Here, we demonstrate that there arises a gapless level attraction in cavity axion polariton of antiferromagnetic topological insulators, which originates from a nonlinear interaction between axion and the odd-order resonance of cavity. Such a novel level attraction is essentially different from conventional level attractions with the mechanism of either a linear coupling or a dissipation-mediated interaction, and also different from the level repulsion induced by the strong coupling in common polaritons. Our results reveal a new mechanism of level attractions, and open up new roads for exploring the axion polariton with cavity technologies. They have potential applications for quantum information and dark matter research.

Introduction. Axion was first postulated as an elementary particle to solve the charge-parity puzzle in the strong interaction between quarks in the particle physics[1]. Now, axion is also considered as a dark matter candidate of the universe[2]. But its existence in nature is another puzzle. Interestingly, axion emerges as a quasiparticle in three-dimensional (3D) topological insulators through the axion action $S_\theta = (\theta/2\pi)(e^2/hc_0) \int d^3x dt \mathbf{E} \cdot \mathbf{B}$ from the topological field theory[3, 4], in which \mathbf{E} and \mathbf{B} are the electromagnetic fields inside the insulators, e is the charge of an electron, h is Plank's constant, θ (modulo 2π) is the dimensionless pseudoscalar parameter as the axion field. The axion field θ can only be 0 for trivial insulators and π for topological insulators because it is odd under the time reversal symmetry \mathcal{T} or the inversion symmetry \mathcal{P} . In antiferromagnetic (AFM) insulators, once both \mathcal{T} and \mathcal{P} are broken, θ can deviate from the quantized values (0 or π) and becomes dynamical due to the spin-wave excitation, denoted as a dynamical axion field (DAF) $\theta(\mathbf{r}, t) = \theta_0 + \delta\theta(\mathbf{r}, t)$ [5–7].

In order to describe the electromagnetic response of 3D topological insulators, the axion action should be included to the conventional Maxwell's action $S_0 = (8/\pi) \int d^3x dt (\epsilon \mathbf{E}^2 - (1/\mu) \mathbf{B}^2)$ to obtain a set of modified Maxwell's equations[8], which indicates DAF naturally couples with the light. Many exotic electromagnetic phenomena were predicted for DAF systems, such as, axion polariton[5], the chiral magnetic effect[9–11], and so on[12–15]. Interestingly, it was also proposed to detect axion dark matter in the universe[16]. But most of them are theoretical studies due to the lack of realistic DAF

materials. Recently, several topological dynamical axion insulators (DAIs) were proposed to host large DAF protected by nonzero spin Chern number[17] and strongly couple with the light, for example, van der Waals(vdW) layered material $\text{Mn}_2\text{Bi}_2\text{Te}_5$ [7] and $\text{MnBi}_2\text{Te}_4/\text{Bi}_2\text{Te}_3$ superlattice[17]. Especially, some of us predicted tunable DAF in MnBi_2Te_4 films[18] which has been successfully synthesized in experiments[19–25]. Detailed discussions on axion materials can also be found in a recent review[26]. Therefore, the cavity with embedded DAI can provide an important platform to study cavity axion polariton induced by the strong coupling between DAF and cavity photon and develop potential applications.

Before turning to cavity axion polariton, we first introduce generic concepts of the level repulsion (LR) and level attraction (LA). As two harmonic oscillators are coherently coupled with strength g_0 , the eigenfrequencies of hybridized modes are repelled with the gap $2g_0$ at resonance, which is known as the LR[27–31], schematically shown in Fig. 1a. When the coupling is of dissipative nature[32–36], a LA may occur, schematically shown in Fig. 1b. The LA spectrum can be generally written as,

$$\omega_{\pm} = \frac{(\omega_a + \omega_b) \pm \sqrt{(\omega_a - \omega_b)^2 - g(\omega)^2}}{2}, \quad (1)$$

where ω_a and ω_b are frequencies of two oscillators a and b , and $g(\omega)$ denotes the coupling strength. Once $|g(\omega)| > |\omega_a - \omega_b|$, the square root gives a pure imaginary value, causing that the real parts of complex frequencies in Eq. (1) are degenerate, i.e. the attraction of mode frequencies. $g(\omega)$ is frequency-independent in most cases,

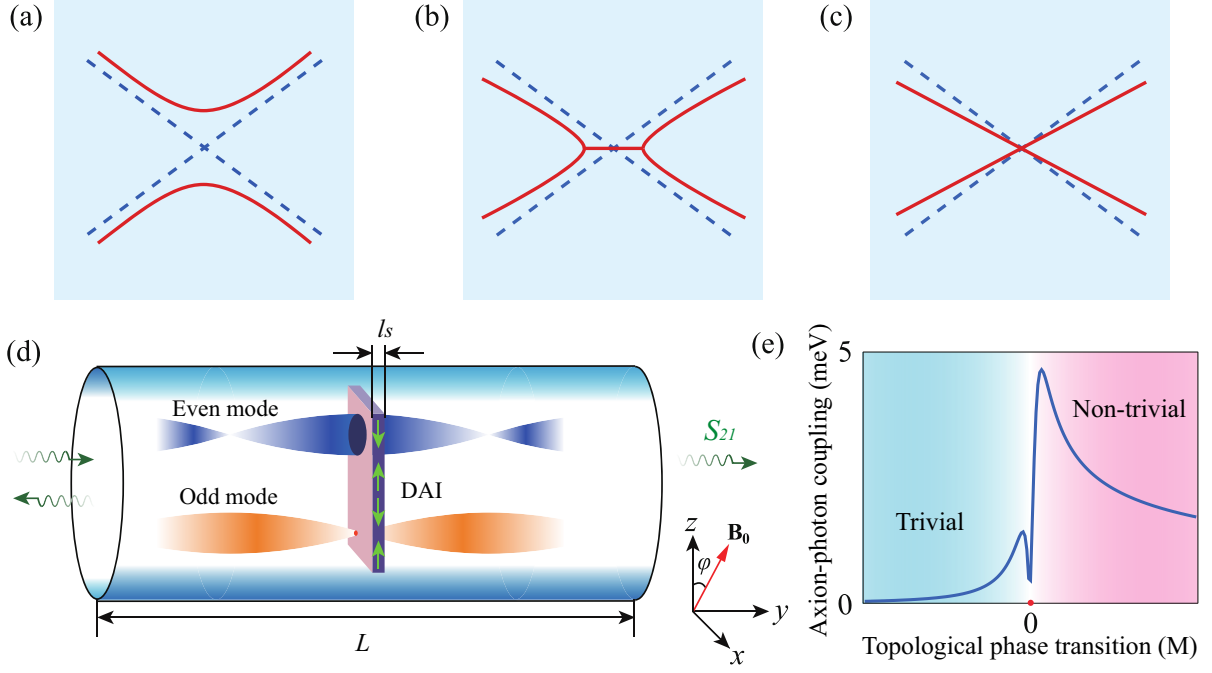


FIG. 1: **Schematic of level repulsion (LR), level attraction (LA), and photon cavity.** **a-c**, Conventional LR (a), conventional LA (b) and unconventional LA (c) depicted with solid red lines. The dashed blue lines generally present two uncoupled modes. **d**, Schematic of photon cavity geometry with a dynamical axion insulator (DAI) film. The photon propagates from the left port to the right port through the DAI film. Depending on the mode number, the cavity resonance mode can be the even mode or the odd mode. As for the odd mode, the electric field at the DAI is negligibly small, indicating that the photon-axion coupling would be dominated by the nonlinear interaction. But for the even mode, a large electric field can lead to a linear photon-axion coupling. The static magnetic field is applied with an angle φ with respect to the z axis and induces the coupling between the electric field \mathbf{E} of photon and dynamical axion field (DAF) $\delta\theta$. **e**, The schematic of the coupling strength between axion mode and the photon mode as a function of the mass parameter M , distinguishing between topologically trivial ($M < 0$) and nontrivial ($M > 0$) DAI.

but it may be frequency dependent, for example, in our system discussed below. In principle, a LA is attributed to various mechanisms, and it has been observed in a few quantum physics, e.g., cavity optomechanics[33] and cavity magnon polariton[34, 35, 37], as well as in classic physics[38], e.g. coupled piano strings. In cavity optomechanics, the Stokes process of photon-phonon interaction results in mechanical amplification and a LA. In cavity magnon polariton, the dissipation mediates the photon-magnon coupling and explicitly induces a LA. Moreover, the phase manipulation of microwave photons can induce a LA in photon-magnon systems as well[39, 40].

In this article, we studied the cavity axion polariton of DAIs and proposed an unconventional LA with a new mechanism. It is achieved by a nonlinear-type strong coupling between DAF and cavity photon. As the coupling strength is greatly enhanced near the topological phase transition, a giant nonlinear axion-photon interaction is induced, producing this unconventional LA and high-order modes. Though the dissipation effect is not the key to producing the LA, it induces a gap of the LA.

Cavity axion polariton. The coupling between photon and DAF in AFM topological insulators can be de-

scribed by the effective action $\mathcal{S}_{\text{tot}} = \mathcal{S}_{\text{Maxwell}} + \mathcal{S}_{\text{topo}} + \mathcal{S}_{\text{axion}}$ [5] (see Supplementary Materials for the details). The dynamics of the coupled DAF and electromagnetic field can be obtained as,

$$\frac{\partial^2 \delta\theta}{\partial t^2} - v^2 \nabla^2 \delta\theta + m^2 \delta\theta + \Gamma \frac{\partial \delta\theta}{\partial t} - \frac{\alpha \mathbf{B}}{8\pi^2 g^2 J} \mathbf{E} = 0, \quad (2)$$

$$\frac{\partial^2 \mathbf{E}}{\partial t^2} - c^2 \nabla^2 \mathbf{E} + \frac{\alpha \mathbf{B}}{\pi \epsilon} \frac{\partial^2 \delta\theta}{\partial t^2} = 0, \quad (3)$$

where $c = c_0/\sqrt{\epsilon\mu}$ with c_0 the speed of light in the vacuum, ϵ and μ represent dielectric constant and magnetic permeability, $\alpha = e^2/\hbar c_0$ is the fine-structure constant, and $\delta\theta$ represents the massive DAF originating from spin-wave mode with material-dependent stiffness J , velocity v_i , mass m , and coefficient g defined in Ref. [5]. $v_i = v$ is assumed to be isotropic, and Γ presents the decay rate of the axion mode.

Furthermore, in the presence of an external uniform magnetic field \mathbf{B}_0 , the coupling strength between the axion mode and the electric field \mathbf{E} of the photon can be derived as $b = \sqrt{\alpha^2 B_{0x}^2 / 8\pi^3 \epsilon g^2 J}$, depending on the x component of \mathbf{B}_0 . As an illustration, we picked representative parameters \mathbf{B}_0 within (0 – 2T) and $\epsilon \sim 20$ for

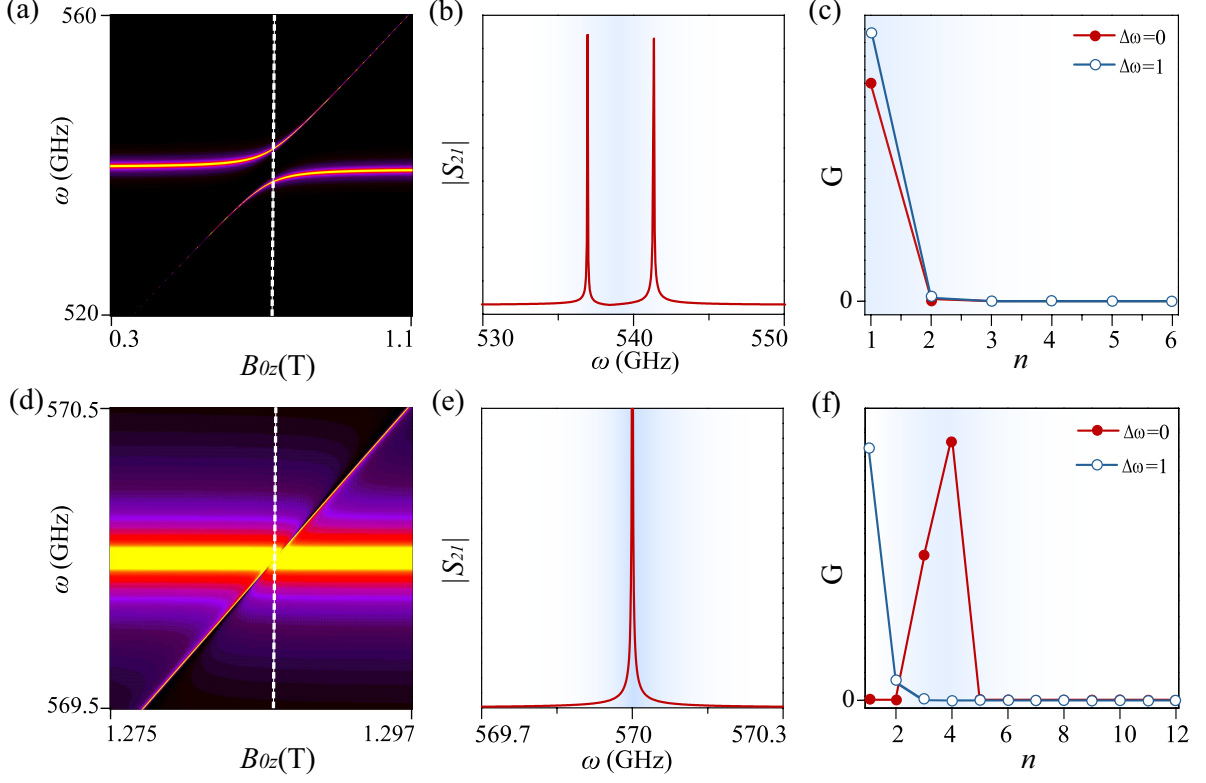


FIG. 2: $|S_{21}|$ **transmission spectra**. **a**, $|S_{21}|$ transmission spectra of the even mode as a function of the static magnetic field and the photon frequency, which is calculated based on Eq. (4) for the DAI film thickness $l_s = 0.1\mu m$. The strong coupling manifests the anticrossing gap. **b**, Spectrum at resonant magnetic field represented by the white dashed line in (a). **c**, Absolute value of the n th-order terms in G . Here, $|S_{21}|$ is formally written as F/G , and G is Taylor-expanded into n th-order terms. As for the even mode, we can see that the linear term ($n=1$) dominates. **d-f**, The same as (a-c) but for the odd mode. In order to avoid divergence, a small imaginary part is added into the frequency ω in Eq. (5). As for the odd mode, the linear term of type-I interaction (represented by $\Delta\omega = 0$) is vanishing. This results in the fact that the high-order terms dominate type-I interaction and generate high-order modes. Moreover, the linear term and second-order term of type-II interaction (represented by $\Delta\omega = 1$) dominate and give rise to Eq. (5).

AFM insulators and the coupling strength b as a function of the mass term M is schematically shown in Fig. 1e. It is distinguished between topologically nontrivial ($M > 0$) and trivial ($M < 0$) DAIs. The magnitude of the coupling strength b in the nontrivial regime is significantly larger than that in the trivial regime. The maximum b can be obtained near the topological transition ($M \sim 0$). Therefore, an AFM topological insulator with a large topological DAF is an ideal candidate for studying strong axion-photon coupling in a cavity.

In order to generate longitudinal magnetization fluctuation δM_z , we consider parallel pumping of antiferromagnet inside a cavity[41]. As shown in Fig. 1d, a DAI is placed in the middle of one-dimensional cylindrical cavity with input and output ports at the left and right ends. The electromagnetic wave propagates along the y axis, the magnetization is aligned along the z axis but the static magnetic field is oriented with the angle φ with respect to the z axis. In this setup, the z magnetic component B_z of the electromagnetic wave induces a periodic

oscillation of magnetization δM_z and thereby establishes a DAF. The x component of external magnetic field \mathbf{B}_0 couples with the electric field E_x and thus contributes to the coupling between the electric field and DAF. Such longitudinal excitation of magnetization is usually referred to parallel pumping. Since parallel pumping is a process that one photon splits into two magnon with the same frequency, we take $m = 2\omega_m$ with $\omega_m = \omega_0 \pm \gamma B_{0z}$ as the AFM resonance frequency, γ is the gyromagnetic ratio and B_{0z} is the z component of \mathbf{B}_0 .

Combining Eqs. (2) and (3) gives rise to the propagation state inside the DAI. With the wave vector \mathbf{k} , one can directly obtain the transfer matrix that connects the electromagnetic field at input port and output port. As for the finite-velocity DAF, the boundary condition needs to be further considered. The scattering matrix and continuity condition at input and output ports are used to calculate transmission coefficient S_{21} . The detailed methods can be seen in Supplementary Material. For our calculations, the axion frequency is $m = 2.07$ meV

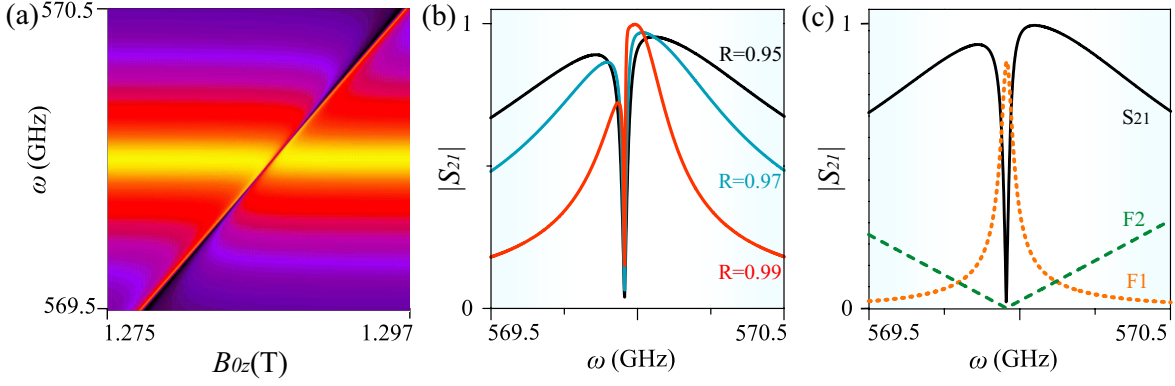


FIG. 3: **Dissipation effect.** **a**, $|S_{21}|$ spectra of the odd mode calculated with full-wave numeric method (without using Taylor expansion) for the DAI film thickness $l_s = 0.1\mu m$ and the reflectivity $R = 0.99$ of the cavity. The reflectivity R of electromagnetic wave at two ports determines the decay rate of intracavity field. **b**, $|S_{21}|$ spectra for the reflectivity $R=0.95$ (black), 0.97 (blue), 0.99 (red) at the resonant magnetic field. As the reflectivity R increases, the dissipation is gradually suppressed, and the gap (dip) width is enhanced little by little. But we notice that the position of the gap remains unchanged. **c**, The schematic mechanism of gaped LA. The approximated formula of $|S_{21}|$ spectra is written as $(\omega - m')/[(\omega - \omega'_c)(\omega - \omega'_1)]$ (S_{21} , black), which can be considered as the combination of two functions $1/[(\omega - \omega'_c)(\omega - \omega'_1)]$ ($F1$, brown) and $(\omega - m')$ ($F2$, green). Here, ' m' ', ' ω'_c ' and ' ω'_1 ' are renormalized by the dissipation. We can see that the function $F2$ (the axion mode) is the key to opening the LA gap.

as $\mathbf{B}_0=0$, thus the cavity resonance frequency is about 0.5 THz and the cavity length is taken to be $L=5$ mm. Depending on the mode number n , the resonance modes of cavity can be either the even mode or the odd mode at the center of the cavity. Strong interaction between the axion mode and the electric field \mathbf{E} , as demonstrated in Eqs. (2) and (3), generates LR between the axion mode and the even mode (see Fig. S1 in Supplementary Material). For the odd mode, our calculations surprisingly present an unconventional LA, seen in Fig. 2.

In order to reveal the origin of such unexpected LA, we derive an analytic expression of transmission spectrum S_{21} , written in the form of $S_{21} = F/G$ (see Supplementary Material for details). The expression of S_{21} is composed of Taylor's expansions around cavity resonance frequency ω_c and the dimension $l_s=0$. The expansion results in two types of interaction, i.e. pure axion interaction (called type-I) and mixed axion-photon interaction (type-II). For the even mode, the type-I interaction dominates and S_{21} can be written as

$$S_{21}^e = C^e \frac{(\omega - m)}{(\omega - \omega_c)(\omega - m) - \eta}, \quad (4)$$

here, C^e denotes a constant and $\eta = \epsilon_r l_s b^2 / 2(L - l_s)$. It well reproduces the characteristic LR (Fig. 2a and 2b), implying the linear coupling between the even mode and the axion mode. This can be further confirmed in Fig. 2c where the linear term is the largest among all terms of G in S_{21} .

But for the odd mode, the the first- and second-order terms of type-I interaction are vanishing (Fig. 2f). As the film thickness l_s is small, the nonlinear type-II interaction mainly contributes to S_{21} . Through simplifying

the function, we reach a compact formula for the odd mode

$$S_{21}^o = C^o \frac{\omega - m}{(\omega - \omega_c)(\omega - \omega_1)}, \quad (5)$$

where C^o also denotes a constant, $\omega_1 = (4m + \lambda\omega_c)/(4 + \lambda)$ and $\lambda = (L - l_s)l_s \epsilon_s b^2 / 2c^2$. From Eq. (5), one can see that there appears a new high-order mode with frequency ω_1 . Since the high-order mode has a smaller slope than the axion mode, it bends to the cavity resonance with an attractive characteristics, shown in Fig. 2d. Moreover, the high-order mode ω_1 reduces to the axion mode at resonance ($m = \omega_c$), reproducing $S_{21} = C^o/(\omega - \omega_c)$ shown in Fig. 2e. Therefore, the LA under this study is of both gapless and nonlinear nature.

Dissipation effects. The reflectivity R indicates the decay rate (dissipation) of photons inside a cavity. A smaller R represents a larger photon leakage (dissipation). In Eq. (5) and Fig. 2, we assume the reflectivity $R=1$, implying no leakage of intracavity photons, and we obtained a gapless LA. Here, we further consider the dissipation ($R < 1$). Figure 3a shows S_{21} spectrum of the odd mode with $R = 0.99$ and a gap at resonance can be clearly seen, different from that gapless LA in Fig. 2d. Furthermore, a larger dissipation (a smaller R) results in a wider gap, shown in Fig. 3b. To understand the behavior in Fig. 3, we deduce an analytic expression of S_{21} in the presence of the dissipation. Interestingly, the new formula is of the same form as Eq. (5). The only difference is that the dissipation of each mode is renormalized, i.e. $\omega'_c = \omega_c - i\eta(1-R)$, $\omega'_1 = \omega_1 - i\zeta(1-R)$ and $m' = m - i\Gamma\omega$. Here, η and ζ are parameters the detailed forms of which are given in Supplementary Materials. The new formula

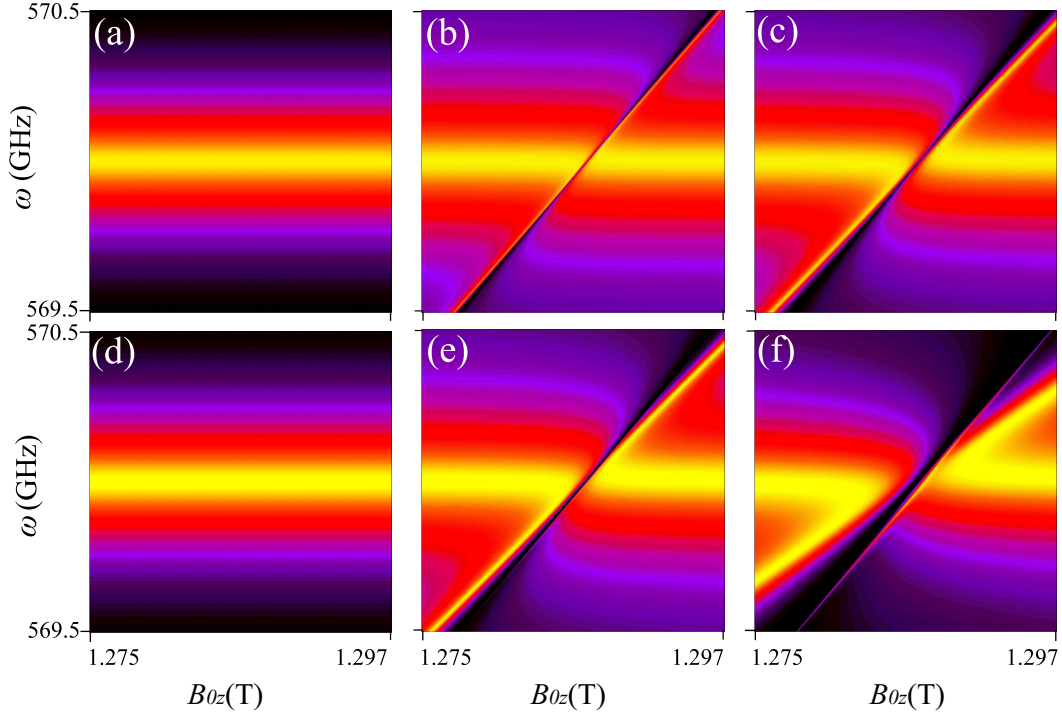


FIG. 4: $|S_{21}|$ transmission spectra dependent on coupling strength and DAI film thickness. **a,b,c**, $|S_{21}|$ spectra for the DAI film thickness $l_s=0.1 \mu\text{m}$ with different coupling strength $b=0$ (**a**), 1(**b**) and 2(**c**) meV. Controllable coupling strength b can be obtained through applying the external magnetic field in topologically nontrivial DAI. We can see that an enhanced gap in LA is induced by a strong coupling. **d-f**, The same as (**a-c**), but for a thicker DAI film $l_s=0.5 \mu\text{m}$. Note that high-order modes arise in the spectrum for which the nonlinear interaction dominates. For all data here, the reflectivity R is fixed to be 0.99.

satisfactorily reproduces the gapped LA (see Supplementary Materials), indicating that the gap originates from the dissipation effect. Further analysis (Fig. 3c) shows that the R -dependent line-width of cavity resonance and high-order mode result in a gap at m , in contrast to the peak (Fig. 2d) in the absence of the dissipation. Therefore, the dissipation is not the key to generating the nonlinear LA, but induces a gap in the LA.

Discussions. The LA found in this work is essentially different from the conventional LA. First of all, the LA here is attributed to a nonlinear interaction, but the conventional LA originates from the linear coupling of two modes[32–35, 37, 39, 40]. Second, the dissipation is not the essence for the LA in this work and it merely tunes the LA gap of the axion polariton. Third, the axion mode under this study arises from longitudinal magnetization fluctuation, instead of transverse magnetization fluctuation in the case of cavity magnon polariton[42–48].

To demonstrate the LA here is controllable, we vary the coupling strength b and the thickness l_s of the DAI film. As shown in Fig. 1e, the topologically trivial DAI possesses negligible axion-photon coupling strength and thus does not couple with cavity resonance (Fig. 4a). Around the topological transition, the coupling strength quickly increases, resulting in a large gap of LA (Fig. 4b

and 4c). This trend of increasing gap can also be obtained through increasing the thickness l_s . But, extra high-order modes may appear. As for a large l_s case, the type-II interaction does not overwhelm the type-I interaction that is absent for a small l_s case. The third-order type-I term which reproduces LR, together with other terms, start to contribute to S_{21} . The high-order terms imply more new modes as shown in Fig. 4e and 4f. The competition between type-I and type-II nonlinear interaction results in the coexistence of LR and LA. Therefore, it is expected to observe LA, LR and nonlinearity-induced high-order modes by tuning the topological phases (M) and the DAI dimension l_s .

To make possible experimental measurement, high-frequency cavity and high-quality DAI materials are important. Recently, Scalari et al. reported the fabrication of μm -size electronic meta-material cavity with resonance frequency up to 4 THz[49]. The ultra-strong coupling with a low dissipation rate have been achieved, implying the potential application in cavity quantum electrodynamics. On the other hand, thanks to the fast-growing field of MnBi_2Te_4 -based magnetic topological materials and state-of-art experimental techniques[19–25], it seems quite promising that candidate materials hosting large topological DAF, such as MnBi_2Te_4 films, $\text{Mn}_2\text{Bi}_2\text{Te}_5$

and $\text{MnBi}_2\text{Te}_4/\text{Bi}_2\text{Te}_3$ superlattice proposed by some of the authors[18, 20], can be realized in the short future and pave the way for the development of cavity axion polariton and potential applications in quantum information and discovery of dark matter in the universe.

Acknowledgements. This work is supported by the Fundamental Research Funds for the Central Universities (Grant No. 020414380149), the Natural Science Foundation of China (Grants No. 61974067, No. 12074181, No. 11674165 and No. 11834006), Natural Science Foundation of Jiangsu Province (No. BK20200007) and the Fok Ying-Tong Education Foundation of China (Grant No. 161006).

* Electronic address: zhanghj@nju.edu.cn

- [1] R. D. Peccei and H. R. Quinn, Phys. Rev. Lett. **38**, 1440 (1977).
- [2] J. Preskill, M. B. Wise, and F. Wilczek, Physics Letters B **120**, 127 (1983), ISSN 0370-2693.
- [3] X.-L. Qi and S.-C. Zhang, Rev. Mod. Phys. **83**, 1057 (2011).
- [4] X.-L. Qi, T. L. Hughes, and S.-C. Zhang, Phys. Rev. B **78**, 195424 (2008).
- [5] R. Li, J. Wang, X. L. Qi, and S. C. Zhang, Nat. Phys. **6**, 284 (2010).
- [6] J. Wang, R. Li, S.-C. Zhang, and X.-L. Qi, Phys. Rev. Lett. **106**, 126403 (2011).
- [7] J. Zhang, D. Wang, M. Shi, T. Zhu, H. Zhang, and J. Wang, Chin. Phys. Lett. **37**, 077304 (2020).
- [8] F. Wilczek, Phys. Rev. Lett. **58**, 1799 (1987).
- [9] A. Sekine and K. Nomura, Phys. Rev. Lett. **116**, 096401 (2016).
- [10] H. Sumiyoshi and S. Fujimoto, Phys. Rev. Lett. **116**, 166601 (2016).
- [11] R. Li, H. Ma, X. Cheng, S. Wang, D. Li, Z. Zhang, Y. Li, and X.-Q. Chen, Phys. Rev. Lett. **117**, 096401 (2016).
- [12] H. Ooguri and M. Oshikawa, Phys. Rev. Lett. **108**, 161803 (2012).
- [13] K. Taguchi, T. Imaeda, T. Hajiri, T. Shiraishi, Y. Tanaka, N. Kitajima, and T. Naka, Phys. Rev. B **97**, 214409 (2018).
- [14] T. Imaeda, Y. Kawaguchi, Y. Tanaka, and M. Sato, J. Phys. Soc. Jpn **88**, 024402 (2019).
- [15] J. Gooth, B. Bradlyn, S. Honnali, C. Schindler, N. Kumar, J. Noky, Y. Qi, C. Shekhar, Y. Sun, Z. Wang, et al., Nature **575**, 315 (2019).
- [16] D. J. E. Marsh, K. C. Fong, E. W. Lentz, L. Šmejkal, and M. N. Ali, Phys. Rev. Lett. **123**, 121601 (2019).
- [17] H. Wang, D. Wang, Z. Yang, M. Shi, J. Ruan, D. Xing, J. Wang, and H. Zhang, Phys. Rev. B **101**, 081109(R) (2020).
- [18] T. Zhu, H. Wang, H. Zhang, and D. Xing, arXiv:2010.05424 (2020).
- [19] Y. Gong, J. Guo, J. Li, K. Zhu, M. Liao, X. Liu, Q. Zhang, L. Gu, L. Tang, X. Feng, et al., Chin. Phys. Lett. **36**, 076801 (2019).
- [20] D. Zhang, M. Shi, T. Zhu, D. Xing, H. Zhang, and J. Wang, Phys. Rev. Lett. **122**, 206401 (2019).
- [21] J. Li, Y. Li, S. Du, Z. Wang, B.-L. Gu, S.-C. Zhang, K. He, W. Duan, and Y. Xu, Sci. Adv. **5**, eaaw5685 (2019).
- [22] M. M. Otrokov, I. I. Klimovskikh, H. Bentmann, D. Estyunin, A. Zeugner, Z. S. Aliev, S. Gass, A. U. B. Wolter, A. V. Koroleva, A. M. Shikin, et al., Nature **576**, 416 (2019).
- [23] Y. Deng, Y. Yu, M. Z. Shi, Z. Guo, Z. Xu, J. Wang, X. H. Chen, and Y. Zhang, Science **367**, 895 (2020).
- [24] C. Liu, Y. Wang, H. Li, Y. Wu, Y. Li, J. Li, K. He, Y. Xu, J. Zhang, and Y. Wang, Nat. Mater. **19**, 522 (2020).
- [25] B. Chen, F. Fei, D. Zhang, B. Zhang, W. Liu, S. Zhang, P. Wang, B. Wei, Y. Zhang, Z. Zuo, et al., Nat. Commun. **10**, 4469 (2019).
- [26] D. M. Neno, C. A. C. Garcia, J. Gooth, C. Felser, and P. Narang, Nat. Rev. Phys. pp. <https://doi.org/10.1038/s42254-020-0240-2> (2020).
- [27] C. Cohen-Tannoudji, J. Dupont-Roc, and G. Grynberg, *Atom-Photon Interactions* (Wiley VCH, New York, 2004).
- [28] M. Aspelmeyer, T. J. Kippenberg, and F. Marquardt, Rev. Mod. Phys. **86**, 1391 (2014).
- [29] G. S. Agarwal, Phys. Rev. Lett. **53**, 1732 (1984).
- [30] Y. Tabuchi, S. Ishino, A. Noguchi, T. Ishikawa, R. Yamazaki, K. Usami, and Y. Nakamura, Science **349**, 405 (2015).
- [31] S. Haroche, Rev. Mod. Phys. **85**, 1083 (2013).
- [32] A. Metelmann and A. A. Clerk, Phys. Rev. X **5**, 021025 (2015).
- [33] N. R. Bernier, L. D. Tóth, A. K. Feofanov, and T. J. Kippenberg, Phys. Rev. A **98**, 023841 (2018).
- [34] M. Harder, Y. Yang, B. M. Yao, C. H. Yu, J. W. Rao, Y. S. Gui, R. L. Stamps, and C.-M. Hu, Phys. Rev. Lett. **121**, 137203 (2018).
- [35] W. Yu, J. Wang, H. Y. Yuan, and J. Xiao, Phys. Rev. Lett. **123**, 227201 (2019).
- [36] Y. Tserkovnyak, A. Brataas, G. E. W. Bauer, and B. I. Halperin, Rev. Mod. Phys. **77**, 1375 (2005).
- [37] B. Bhoi, B. Kim, S.-H. Jang, J. Kim, J. Yang, Y.-J. Cho, and S.-K. Kim, Phys. Rev. B **99**, 134426 (2019).
- [38] G. Weinreich, The Journal of the Acoustical Society of America **62**, 1474 (1977).
- [39] V. L. Grigoryan, K. Shen, and K. Xia, Phys. Rev. B **98**, 024406 (2018).
- [40] I. Bovenster, C. Dörflinger, T. Wolz, R. Macêdo, R. Lebrun, M. Kläui, and M. Weides, Phys. Rev. Research **2**, 013154 (2020).
- [41] F. R. Morgenthaler, Phys. Rev. Lett. **11**, 69 (1963).
- [42] O. O. Soykal and M. E. Flatté, Phys. Rev. Lett. **104**, 077202 (2010).
- [43] H. Huebl, C. W. Zollitsch, J. Lotze, F. Hocke, M. Greifenstein, A. Marx, R. Gross, and S. T. B. Goennenwein, Phys. Rev. Lett. **111**, 127003 (2013).
- [44] Y. Tabuchi, S. Ishino, T. Ishikawa, R. Yamazaki, K. Usami, and Y. Nakamura, Phys. Rev. Lett. **113**, 083603 (2014).
- [45] M. Goryachev, W. G. Farr, D. L. Creedon, Y. Fan, M. Kostylev, and M. E. Tobar, Phys. Rev. Applied **2**, 054002 (2014).
- [46] X. Zhang, C.-L. Zou, L. Jiang, and H. X. Tang, Phys. Rev. Lett. **113**, 156401 (2014).
- [47] L. Bai, M. Harder, Y. P. Chen, X. Fan, J. Q. Xiao, and C.-M. Hu, Phys. Rev. Lett. **114**, 227201 (2015).
- [48] Y.-P. Wang, G.-Q. Zhang, D. Zhang, T.-F. Li, C.-M. Hu, and J. Q. You, Phys. Rev. Lett. **120**, 057202 (2018).

- [49] G. Scalari, C. Maissen, D. Turčinková, D. Hagenmüller, S. De Liberato, C. Ciuti, C. Reichl, D. Schuh, W. Wegscheider, M. Beck, et al., *Science* **335**, 1323 (2012).